Effect of Hierarchical Deformable Motion Compensation on Image Enhancement for DSA Acquired via C-ARM

Liyang Wei[1], Dinggang Shen[2], Dinesh Kumar[1], Ram Turlapati[3], Jasjit S. Suri[1]
[1]Eigen LLC, 13366 Grass Valley Ave, Grass Valley, CA, 95945
[2]Department of Radiology, University of Pennsylvania School of Medicine, PA, 19104
[3]Theda Clark Hospital, Appleton, University of Wisconsin, WI, 54911

ABSTRACT

DSA images suffer from challenges like system X-ray noise and artifacts due to patient movement. In this paper, we present a two-step strategy to improve DSA image quality. First, a hierarchical deformable registration algorithm is used to register the mask frame and the bolus frame before subtraction. Second, the resulted DSA image is further enhanced by background diffusion and nonlinear normalization for better visualization.

Two major changes are made in the hierarchical deformable registration algorithm for DSA images: 1) B-Spline is used to represent the deformation field in order to produce the smooth deformation field; 2) two features are defined as the attribute vector for each point in the image, i.e., original image intensity and gradient. Also, for speeding up the 2D image registration, the hierarchical motion compensation algorithm is implemented by a multi-resolution framework.

The proposed method has been evaluated on a database of 73 subjects by quantitatively measuring signal-to-noise (SNR) ratio. DSA embedded with proposed strategies demonstrates an improvement of 74.1% over conventional DSA in terms of SNR. Our system runs on Eigen's DSA workstation using C++ in Windows environment.

Keywords: DSA, Hierarchical deformable registration, Diffusion, Nonlinear normalization

1. INTRODUCTION

Digital subtraction angiography (DSA) is a well-established modality for visualization of blood vessels in the human body [1]. Ideally, the DSA image mainly contains the dye-enhanced blood vessels, which appear dark. But in reality, the image quality suffers from challenges like system noise and motion artifacts due to patient movement. In [2], Wei *et al* proposed a nonlinear normalization technique to enhance blood vessels. In this paper, we further propose a two-step strategy for DSA images: (1) first compensates the motion artifacts by a hierarchical deformable registration algorithm, and (2) enhances the registered DSA image by anisotropic diffusion and nonlinear normalization techniques.

Image registration is a procedure of finding a spatial deformation that describes point-wise correspondence between a pair or a group of images. There are numerous applications in the areas of medical image analysis [3]-[5]. Here, a hierarchical deformable registration method is applied to registering DSA images and further removing the motion artifacts due to patient movement. It is an extension of the method in [3], which was originally developed for 3D Brain image registration. Two major changes are made here for DSA images, i.e., B-Spline to represent the deformation field and new attribute vectors to match correspondences. Also, multi-resolution framework is used to speed up the registration procedure.

DSA image is then obtained by subtraction between registered bolus image and mask image. A diffusion technique and a nonlinear normalization method are subsequently applied to improving image quality. In particular, a diffusion technique, based on anisotropic diffusion proposed by Perona and Malik [6], is first used to effectively remove the background noise, without destroying the vessels and translucency of the contents inside the vessels in DSA images (This technique relies on the diffusion flux to iteratively eliminate small variations due to noise and preserve large variations due to edges; and it has been widely applied to ultrasound denoising [7, 8] and other medical images [9]). The nonlinear normalization is applied to post diffused DSA images. It classifies the DSA image into foreground and background regions and weights them differently.

Image Processing: Algorithms and Systems VI, edited by Jaakko T. Astola,
Karen O. Egiazarian, Edward R. Dougherty, Proc. of SPIE-IS&T Electronic Imaging,
SPIE Vol. 6812, 68120Z, © 2008 SPIE-IS&T · 0277-786X/08/$18

The paper is organized as follows. Section 2 discusses the principle of the motion compensation and image enhancement algorithms. The experiment setup and performance evaluation are presented in Section 3. Section 4 demonstrates results on clinical data. Finally, conclusions are drawn in Section 5.

2. METHODOLOGY

For acquiring DSA images, two steps are generally performed. First, a series of frames, referred as mask frames, are taken to represent the body anatomy in static form. Then, after the dye is injected into the human body to visualize the blood vessel, a second series of frames, called bolus frames, are acquired. In the conventional DSA, all mask frames and bolus frames are respectively averaged to reduce noise in the images, and a subtraction procedure is directly preformed between the averaged bolus frame and the averaged mask frame to generate the DSA image. Since there exist possible body movements between bolus frames and mask frames, the direct subtraction might lead to artifacts in the DSA images.

In this paper, we first register the averaged mask frame with averaged bolus frame, to minimize the motion artifacts before subtraction. Then, using registered DSA image as input, we use an anisotropic diffusion technique to reduce noise, followed by a nonlinear normalization method to enhance the blood vessel. We will detail each of these steps in the following.

2.1 Hierarchical Motion Compensation

The hierarchical motion compensation algorithm proposed here is an extension of HAMMER registration algorithm in [3]. Two major improvements are made for DSA images. First, a B-spline basis function [4] is applied to represent the deformation field, in order to produce the smooth deformation field without the need of point-wise deformation smoothing in each iterative registration procedure. Second, two features are particularly defined as the attribute vector for each point in the image, i.e., original image intensity and gradient. Also, for speeding up the 2D image registration, the hierarchical motion compensation algorithm is implemented by a multi-resolution framework.

The energy function of our hierarchical motion compensation algorithm is defined as follows:

$$E(T)=\sum_{v\in\Omega}(F(v)-M(T(v)))^2+\lambda(|\nabla F(v)|-|\nabla M(T(v))|)^2 \tag{1}$$

In Eq. (1), v is a pixel in the fixed image domain. The first energy item measures the image intensity difference. $F(v)$ is the intensity of pixel v in the fixed image, and $M(T(v))$ is the intensity of the corresponding pixel in the moving image. $T(\,)$ represents the deformation of pixel v. The second energy item in (1) measures the gradient difference between two images. $|\nabla F(\,)|$ and $|\nabla M(\,)|$ are the gradient magnitudes of the fixed and the moving images, respectively. λ is the weight which balances the intensity differences and the gradient differences between the two images. The goal of the registration is to find a deformation $T(\,)$ by minimizing the energy function in Eq. (1).

The deformation $T(\,)$ defines the pixel-wise displacements from the fixed image onto the moving image. In this paper, we apply a B-Spline based model to describe the deformation $T(\,)$. Compared with other splines and basis functions, B-splines are locally controlled and computationally efficient.

B-Spline deformation model uses a number of regularly distributed control points to represent the deformation. The basic idea of the free-form deformation (FFD) [4] based on B-splines is to deform an object by manipulating an underlying mesh of control points. To define a spline-based FFD, the domain of the image region is denoted as $\Omega=\{(x,y)\,|\,0\le x\le X, 0\le y\le Y\}$. Let Φ denote a $n_x\times n_y$ mesh of control points $\phi_{i,j}$ with uniform spacing δ_t. Then, the FFD can be written as follows:

$$T(x,y)=\sum_{m=0}^{3}\sum_{n=0}^{3}B_m(u)B_n(v)\phi_{i+m,j+n} \tag{2}$$

where $i=\lfloor x/n_x\rfloor-1$, $j=\lfloor y/n_y\rfloor-1$, $u=x/n_x-\lfloor x/n_x\rfloor$, $v=y/n_y-\lfloor y/n_y\rfloor$. B_m represents the *m*th basis function of the B-spline (defined as follows):

$$B_0(u) = (1-u)^3/6\,,\; B_1(u) = (3u^3 - 6u^2 + 4)/6\,,$$
$$B_2(u) = (-3u^3 + 3u^2 + 3u + 1)/6\,,\; B_3(u) = u^3/6 \tag{3}$$

Once the grids of control points are given, the purpose of the registration is to determine the location of every control point so that the interpolated deformation $T(\,)$ can minimize the energy function defined in Eq. (1). The optimization method is gradient descent, and the method to estimate the gradient of energy function is the finite differential method.

Suppose there is a control point c, and its coordinates are c_x, c_y, we calculate the following energy functions according to the finite differential method in order to determine the gradient of the objective function:

$$E(c_x, c_y)\,,\; E(c_x+\delta, c_y)\,,\; E(c_x-\delta, c_y)\,,\; E(c_x, c_y+\delta)\,,\; E(c_x, c_y-\delta) \tag{4}$$

where δ is a step value. If $E(c_x, c_y)$ is smallest among all five energy functions, the control point will not be moved. For other cases, we calculate the gradient as follows,

$$\frac{\partial E}{\partial c_x} = \frac{E(c_x+\delta, c_y) - E(c_x-\delta, c_y)}{2\delta} \tag{5}$$

$$\frac{\partial E}{\partial c_y} = \frac{E(c_x, c_y+\delta) - E(c_x, c_y-\delta)}{2\delta} \tag{6}$$

Here, we use $\delta c_x = \frac{\partial E}{\partial c_x} / \left|\frac{\partial E}{\partial c_x}\right|$ and $\delta c_y = \frac{\partial E}{\partial c_y} / \left|\frac{\partial E}{\partial c_y}\right|$ to update the control point c_x, c_y: $c_x = c_x - \mu\delta c_x$ and $c_y = c_y - \mu\delta c_y$, where μ is a step size.

The proposed registration method is performed under a multi-resolution framework, in order to obtain more robust results and fasten the registration procedure. In this case, the two images F and M are first down-sampled into several resolutions. The registration procedure is first performed on the low resolution images. After this, the deformation fields estimated from the low resolution images are up-sampled and used as an initialization for the registration of higher resolution images. By repeating this procedure, we can finally complete the registration for the highest resolution images.

The method here also follows a hierarchical strategy, i.e., the hierarchical selection of control points (regions) to perform image matching. We classify the image region (or the control points) into two groups, one is the region where the local similarity of the two images is large and the other is where the local similarity is small. Since the image regions in the second group are already matched, during each iteration we thus only update the control points in the first group, while remain the control points in the second group unchanged. Using this strategy, we not only speed up the registration procedure, but also prevent artifacts in the image regions with small differences.

2.2 Image Enhancement

After image registration, subtraction is performed between the registered mask image and bolus image, resulting in the motion compensated (registered) DSA image. Using the registered DSA image as input, we further reduce noise and enhance the blood vessel by an anisotropic diffusion technique and a nonlinear normalization method as detailed next.

2.2.1. Anisotropic Diffusion

The anisotropic diffusion technique was proposed by Perona and Malik [6], and is based on partial differential equation (PDE) for noise smoothing. Given an image $I(x, y, t)$ at time scale *t*, the diffusion process is expressed as:

$$\frac{\partial}{\partial t} I(x,y,t) = div(c(x,y,t)\nabla I) \tag{7}$$

where ∇ is the gradient operator, div is the divergence operator, and $c(x,y,t)$ is the diffusion coefficient at location (x,y) at time *t*. By applying the divergence operator, Eq. (7) can be rewritten as

$$\frac{\partial}{\partial t} I(x,y,t) = c(x,y,t)\Delta I + \nabla c(x,y,t)\nabla I \tag{8}$$

where Δ is the Laplacian operator. The diffusion coefficient $c(x,y,t)$ is the key in the smoothing process and it should encourage homogenous-region smoothing and inhibit the smoothing across the boundaries. It is chosen in [6] as a function of the magnitude of the gradient of the brightness function, i.e.,

$$c(x,y,t) = g(\|\nabla I(x,y,t)\|) \tag{9}$$

The suggested functions for $g(\bullet)$ are the following two,

$$g(\nabla I) = e^{-(\frac{\|\nabla I\|}{K})^2} \quad \text{or} \quad g(\nabla I) = \frac{1}{1+(\frac{\|\nabla I\|}{K})^2} \tag{10}$$

where K is the diffusion constant which controls the edge magnitude threshold. Generally speaking, a larger K produces a smoother result in a homogenous region than a smaller K. Here, we apply a diffusion technique on the registered DSA images to smooth background, thereby reducing the structured noise.

2.2.2 Nonlinear Normalization

Following diffusion, we then apply a two-class nonlinear normalization method [2] over diffused DSA images. The principle is to force the background to suppress the non-vascular structures and noise, while gradually enhancing the foreground vascular structures. This concept is implemented as a LUT table where the output pixel is a function of input pixel.

Let $I_{in}(x,y)$ be the input DSA image (after diffusion). The output DSA image after nonlinear normalization, denoted as $I_{out}(x,y)$, can be mathematically obtained as:

$$I_{out}(x,y) = \begin{cases} I_t\left(\dfrac{I_{in}(x,y)}{I_t}\right)^{y_1}, \ I_{in}(x,y) \in [0, I_t] \\ (I_t+1)+(I_t+1)\left(\dfrac{I_{in}(x,y)-(I_t+1)}{I_t+1}\right)^{y_2}, \ \mathrm{I}_{in}(x,y) \in [I_t+1, 255] \end{cases} \tag{11}$$

Here, I_t is a pre-defined threshold, y_1>1.0 and y_2 <1.0 for class-based contrast enhancement. So, if the intensity range of dye lies in lower half of the image and the background lies in the higher half of the image, the blood vessels are enhanced in limits.

3. EXPERIMENT SETUP AND PERFORMANCE EVALUATION

3.1 Data Acquisition

The clinical dataset used here was collected from 73 patients and includes DSA images of Carotid, Renal and Neural. OEC9800 C-Arms is used as X-ray imaging system (rotating anode X-ray tube 0.3mm & 0.6mm). The Innova 2000 dose per frame varies according to the frame rate (7.5 fps - 24 millirad/frame; 15 fps - 18 millirad/frame; 30 fps - 11 millirad/frame). The actual dose varies with patient size and anatomy being imaged.

3.2 Performance Evaluation

The image quality is evaluated in terms of signal-to-noise ratio (SNR) [10, 11]. SNR is defined as in Eq. (12): the ratio of the mean of intensity difference between the signal (foreground) and the noise (background) to the standard deviation of the noise.

$$SNR = \left| \frac{\mu_{signal} - \mu_{noise}}{\sqrt{2}\sigma_{noise}} \right| \tag{12}$$

In DSA image, signals are the visualized blood vessels and noises are the background regions in the image. We choose small signal window (contains blood vessels) and noise window (mainly contains background) in each image, and compute mean and standard deviation based on pixel intensity value in the windows (range from [0,255] for gray image) to get final SNR.

4. RESULTS

As we discussed in Section 2, hierarchical motion compensation, anisotropic diffusion, and nonlinear normalization algorithms are all associated with some pre-defined parameters. Table 1 shows the default values of the parameters selected in this paper. These values were selected empirically over 73 datasets.

Table. 1. Default Values of the Parameters

Hierarchical Motion Compensation	iteration=6 (high resolution), 10 (middle resolution), 30 (low resolution); μ=0.75 (high), 0.45 (middle), 0.08 (low);
Diffusion	t=0.02; K=4.0; n (iteration number)=500
Nonlinear Normalization	I_t=127; y_1=2.0; y_2=0.8;

We tested our proposed method using the clinical dataset described in Section 3. Three typical examples are shown in Figure 1. From the top to the bottom row, there are iliac, neural, and renal images, respectively. Each row includes the conventional DSA image (a), the motion corrected DSA image (b), and the enhanced motion corrected image (c) from the same subject. For each example, we can clearly see that the background structures are minimized after registration (the image (b) in each row). Moreover, in the image (c), the blood vessels are further enhanced and better visualized based on the registered DSA.

The results between different methods are further evaluated by SNR measurement. Table 2 shows the SNR measurement by different methods. The results are obtained by averaging all 73 patients. We chose small signal and noise windows (window size 41x41) on each image to compute SNR; and the same windows were selected for all images from the same subject. From Table II, we can see that the registration step can improve SNR for 18.5% compared with conventional DSA, and the combined registration and enhancement step can improve SNR for 74.1% compared with conventional DSA. Especially, for the 39 "motion obvious" subjects in the dataset, our two-step (registration and enhancement combined) strategy can improve SNR around 39.6% compared with one step (enhancement only) strategy on average.

Table. 2. Results Evaluated by SNR

	Conventional DSA	Motion-corrected DSA	Motion-corrected DSA with Enhancement
SNR	3.39	4.02	5.91
Improvement	-	18.5%	74.1%

5. CONCLUSION

In this paper, we presented a new combined registration and enhancement strategy to improve DSA image quality. First, the motion artifacts are minimized by hierarchical motion compensation using a deformable image registration algorithm. Second, anisotropic diffusion and nonlinear normalization techniques are subsequently applied for noise reduction and blood vessels enhancement. The proposed combined registration and enhancement strategy has been evaluated on a clinical database with brain, renal and carotid images. It was shown that DSA embedded with our combined registration and enhancement strategy could improve SNR for 74.1% compared with conventional DSA.

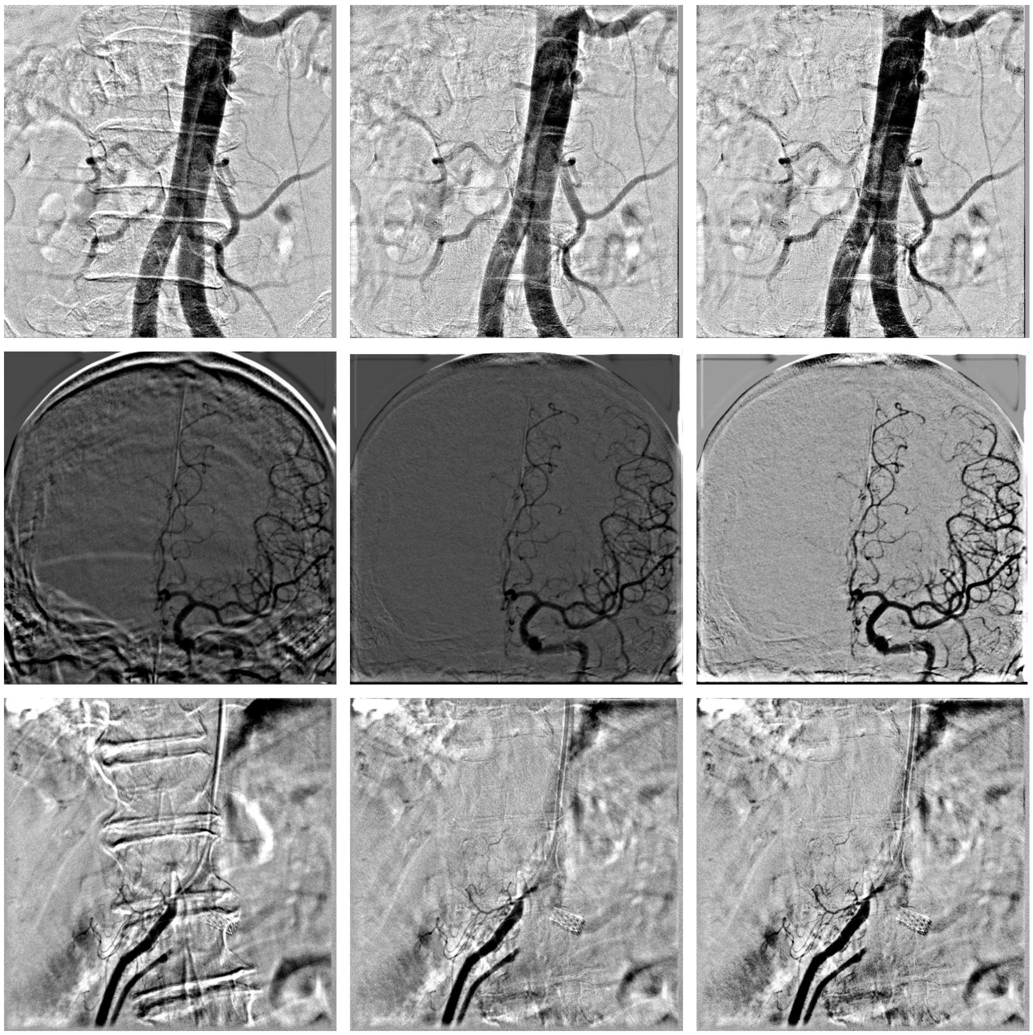

(a) Conventional DSA (b) Motion corrected DSA (c) Enhancement on (b)

Fig. 1. Comparisons on (a) conventional DSA images, (b) motion corrected DSA images, (c) enhancement on motion corrected DSA images, for iliac (Top row), neural (Middle row), and renal images (bottom row).

REFERENCES

1. R. A. Kruger and S. J. Riederer, *Basic concepts of digital subtraction angiography*, Mosby-Year Book Inc, 1984.

2. L. Wei, D. Kumar, J. Coleman, R. Turlapthi and J. S. Suri, "Class-based nonlinear enhancement strategy and its validation: an application for digital subtraction angiography (DSA)," *Proceeding (555) Biomedical Engineering, BioMed*, Austria, 2007.
3. D. Shen and C. Davatzikos, "HAMMER: Hierarchical attribute matching mechanism for elastic registration," *IEEE Trans on Medical Imaging*, Vol. 21, pp. 1421-1439, 2002.
4. D. Rueckert, L.I. Sonoda, C. Hayes, D.L.G. Hill, M.O. Leach, and D.J. Hawkes, "Non-rigid registration using free-form deformations: Application to breast MR images," *IEEE Trans on Medical Imaging*, Vol. 18, pp. 712-721, 1999.
5. D. Forsey and R. Bartels, "Hierarchical B-Spline Refinement," *ACM SIGGRAPH Computer Graphics*, Vol. 22, No. 4, pp. 205-212, Aug. 1988.
6. P. Perona and J. Malik, "Scale-space and edge detection using anisotropic diffusion," *IEEE Trans. Pattern Anal. Mach. Intell.*, Vol. 12, No. 7, pp. 629-639, 1990.
7. Y. Yu and S.T. Acton, "Speckle reducing anisotropic diffusion," *IEEE Trans. Image Process.*, Vol. 11, No. 11, pp. 1260-1270, 2002.
8. S. Aja-Fernandez and C. Alberola-Lopez, "On the estimation of the coefficient of variation for anisotropic diffusion speckle filtering," *IEEE Trans. Image Process.*, Vol. 15, No. 9, pp. 2694-2701, 2006.
9. J.S. Suri and S. Laxminarayan, *PDE and Level Sets: An application to static and motion imagery*, Kluwer Academic/ Plenum Publishers, 2002.
10. J.S. Suri, Y. Guo, C. Coad, T. Danielson, I. Elbakri and R. Janer, "Image quality assessment via segmentation of breast lesion in X-ray and ultrasound phantom images from Fischer's full field digital mammography and ultrasound system," *Technology in Cancer Research & Treatment*, Vol. 4, No. 1, pp. 1-9, 2005.
11. E. Madsen, J. Zagzebski, G. Frank and J. Rownd, *Automated system and method for testing resolution of ultrasound scanners*, Patent US 5,574, 212 (1996).